Theor Chem Acc (2012) 131:1202
DOI 10.1007/s00214-012-1202-2

FEATURE ARTICLE

Some recent developments in photoelectrochemical water splitting using nanostructured TiO_2: a short review

Paul Szymanski · Mostafa A. El-Sayed

Received: 17 January 2012 / Accepted: 3 March 2012 / Published online: 30 May 2012

Abstract Photoelectrochemical cells with TiO_2 electrodes to convert sunlight and water into gaseous hydrogen and oxygen are a source of clean and renewable fuel. Despite their great potential, far-from-ideal performance and poor utilization of the solar spectrum have prevented them from becoming a widespread and practical technology. We review recent experimental work that uses dynamics measurements to study limitations of photoelectrochemical cells from a fundamental level and the use of TiO_2 nanotube arrays as a superior alternative to TiO_2 nanoparticles. Through a combination of nanoscale size control, doping, composite materials, and the incorporation of noble-metal nanoparticles, improved performance and light harvesting are demonstrated.

Keywords Titanium dioxide · Nanotubes · Transient absorption · Plasmonics · Solar energy · Hydrogen · Photoelectrochemistry

Abbreviations

AM 1.5 G	Air mass 1.5 global
FDTD	Finite-difference time-domain
NP	Nanoparticle
NT	Nanotube
PEC	Photoelectrochemical
SPR	Surface plasmon resonance
TA	Transient absorption
XPS	X-ray photoelectron spectroscopy

Dedicated to Professor Marco Antonio Chaer Nascimento and published as part of the special collection of articles celebrating his 65th birthday.

P. Szymanski · M. A. El-Sayed (✉)
Laser Dynamics Laboratory, Georgia Institute of Technology, School of Chemistry and Biochemistry, Atlanta, GA 303332, USA
e-mail: melsayed@gatech.edu

1 Introduction

It gives me a special and great pleasure to contribute a review type manuscript honoring the great contributions of an excellent theorist and a long-time close friend, Professor Nascimento. Soon after his studies at Cal Tech, Marco made excellent and well-recognized theoretical contributions to the field of nonlinear spectroscopy, in which my group and I were working on from the experimental side. We learned a great deal from his papers and from interacting with him on a personal level. He was always willing to help in an effective way in explaining the theoretical basis of his important work. We became very good friends. I very much enjoyed my visit to Rio a number of years ago, mostly because of the great hospitality of Marco and his family and my scientific interaction with Marco and his group. I do wish him and his family a healthy and enjoyable future.

Green and efficient energy technologies are a key area where nanoscience could accelerate the transition from fossil fuels to renewable energy sources. One attractive possibility is conversion of solar energy to electricity or chemical fuel. Sunlight is an abundant and free energy source, which can provide the earth's surface with an amount of energy equivalent to that consumed by the whole world's population in an entire year in just 1.5 h [1]. Semiconductor nanomaterials may play a prominent role as they can function as photocatalysts promoting various oxidation and reduction reactions under sunlight [2].

One of the primary research and technology areas, the use of metal oxide nanomaterials in dye-sensitized solar

cells to generate electricity, is not covered here. We instead focus on the related problem of "water splitting"—harnessing solar energy to obtain hydrogen and oxygen from water—through a combination of photocatalysis and electrochemistry. We emphasize recent developments in optimizing the growth of TiO_2 nanotubes to improve their catalytic properties, new strategies toward combining TiO_2 with other semiconductors to form higher-performance composite materials, the use of plasmonics to increase device efficiency and the ongoing work to gain a detailed understanding of the underlying mechanisms and dynamics in TiO_2 photocatalysis. Although this review is dedicated to experimental work, we hope that it will prove inspiring and informative to the theoretical community.

Hydrogen is an attractive potential fuel source for future vehicles and other applications. Unlike fossil fuels, combustion of H_2 liberates energy without releasing carbon dioxide into the atmosphere. In order for hydrogen to meet the demand for a fuel that has minimal impact on the environment, significant amounts of highly pure H_2 are required. As such sources are not found in nature, they must be produced artificially. In the ideal case, "water splitting" could provide a supply of pure H_2. As combustion of pure H_2 produces only water vapor, it would qualify as renewable energy if the fuel production could be powered by an abundant and non-polluting energy source.

One particularly promising approach is photoelectrochemical (PEC) water splitting as it was first demonstrated by Fujishima and Honda [3]. This method spatially separates water oxidation (producing O_2) and hydrogen reduction (producing H_2) by having each process occur at a separate electrode (Fig. 1). Light absorption by a semiconductor electrode provides energy for the reaction,

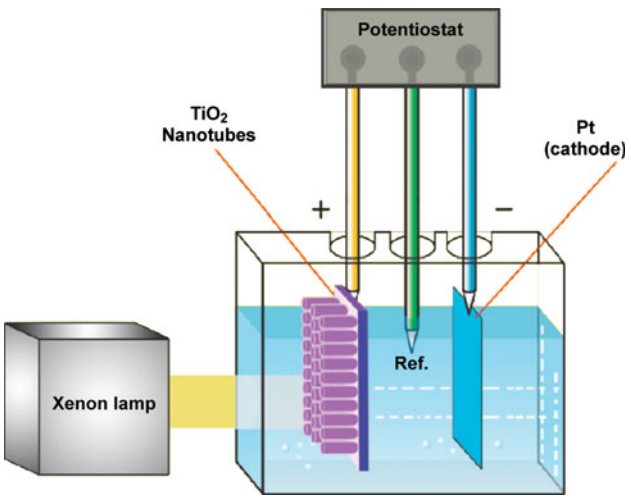

Fig. 1 Schematic of a three-electrode (anode, cathode, and reference electrode) photoelectrochemical (PEC) cell, employing TiO_2 nanomaterials in the anode. Reprinted with permission from Hamedani et al. [36]. Copyright 2011 American Chemical Society

assisted by an applied (electrical or chemical) bias to compensate for insufficient PEC cell voltage and overcome slow kinetics (in electrochemical nomenclature, the additional voltage required to drive a reaction at a desired rate or current density is known as *overpotential*). In an efficient system, the energy stored as fuel (H_2) will exceed the energy consumed by applying the bias.

Fujishima and Honda used an anode of bulk TiO_2 in their PEC cell. Modern designs typically make use of inexpensive TiO_2 nanoparticles (NPs), spread onto a conductive substrate and sintered to form a thin mesoporous film [4], similar to what is used in dye-sensitized solar cells [5]. Although the band gap of TiO_2 only allows absorption of UV light, comprising $\sim$4 % of the solar spectrum, the combination of low cost and chemical stability has proved difficult to surpass in other materials [6]. The efficiency of converting the energy from incident light to H_2 fuel, however, is less than 0.4 % [7] taking into account the entire air mass 1.5 global (AM 1.5 G, $\sim$100 mW/cm^2) solar spectrum [8]. Even considering only the spectrum from 320 to 400 nm around the TiO_2 absorption edge, a PEC made using TiO_2 NPs is at best $\sim$12 % efficient [7]. This is clearly far from ideal, and given the numerous advantages of TiO_2, multiple strategies have been employed to improve upon the original design.

As we will demonstrate, engineering the size and shape of nanoscale TiO_2 can have a significant impact on the conversion efficiency. To better understand the origin of these effects, we first discuss in more detail the mechanism of water splitting to uncover what fundamentally limits the efficiency. As another means of improving performance, incorporating other elements into the TiO_2 crystal lattice can enable the PEC to respond to visible light and we give examples of this in Sect. 4. Integrating advances made in another field of nanoscience, plasmonics has great promise to improve efficiency even further, which is discussed in Sect. 5. We conclude with some thoughts on future research directions in the field of PEC hydrogen production from water.

2 Mechanistic studies

Despite numerous studies of the catalytic efficiency of TiO_2 and other materials and the electron dynamics within photoexcited TiO_2, the mechanism of the water splitting itself has not been widely investigated. Because of the possibly long lifetimes of the photoelectrons and photoholes, the competing process of electron–hole recombination, and surface modifications that may occur when the catalyst is exposed to light for an extended duration, these measurements are extremely challenging to perform [4]. All of the results highlighted in this section used anodes

containing TiO_2 NPs; however, it is expected that the findings will provide insight into the behavior of other nanostructures such as nanotubes (NTs).

Transient absorption (TA) spectroscopy has greatly improved our understanding of solar-powered devices, particularly in the areas of photocatalysis and photovoltaics using TiO_2. In the technique, a "pump" pulse, typically from a laser, places the sample in an excited state with new electronic and/or chemical properties. A time-delayed "probe" pulse measures the absorption spectrum of the sample after it is altered by the first pulse. Measuring the change in absorption compared to the initial value as a function of the delay between the pulses gives the dynamics of the system (Fig. 2).

When TiO_2 is photoexcited with energies greater than its band gap, an electron–hole pair, or exciton, is created. The electron and hole each become trapped at the surface within $\sim$200 fs, giving rise to broad absorption features in the visible and near-IR regions of the spectrum [9]. Electrons gradually diffuse from these "shallow trap" states into lower-energy states within the bulk, causing absorption that is weak in the near-IR but grows increasingly more intense as the wavelength increases [9]. The induced absorption from the photoelectrons and photoholes is observed readily in TA experiments.

In all dynamics measurements meant to mimic the effects of sunlight, it is important to keep the incident laser fluence low. For example, Murai et al. [10] detect TA signals for electrons and holes in TiO_2 that decay at similar rates at fluences up to 0.28 mJ cm^{-2}. These weak excitation densities correspond to an average of one electron–hole pair or less per nanoparticle. At 3.4 mJ cm^{-2}, far above fluences produced by sunlight, the NPs relax much more rapidly. The results suggest bulk recombination of electron and holes begins to dominate once a sufficient density of electron–hole pairs is generated.

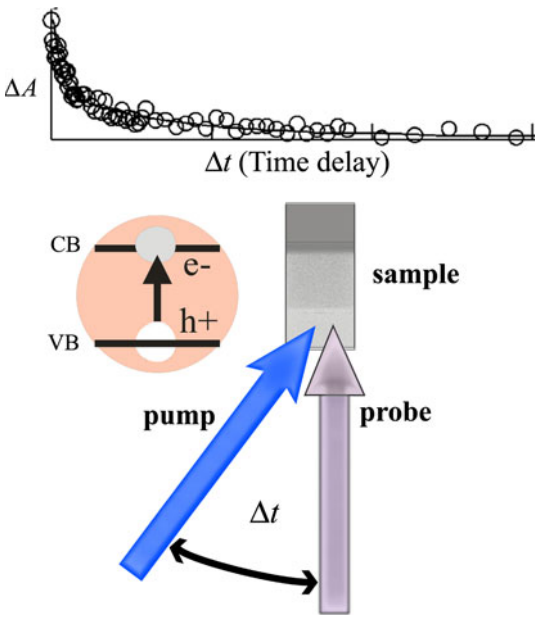

Fig. 2 Pump-probe transient absorption (TA) spectroscopy

Under open-circuit conditions, there is little or no oxygen evolution [4] or change in the photoelectron and photohole dynamics [10] when TiO_2 NPs in water are irradiated by UV light. This is strong indirect evidence that water splitting is much slower than electron–hole recombination.

To obtain direct evidence, recombination must be suppressed in a functioning PEC cell. One strategy is to introduce a scavenger species to rapidly remove either electrons or holes from the vicinity of the TiO_2. In work by Tang et al. [11], the film of TiO_2 NPs is immersed in $AgNO_3$ solution rather then pure water, and Ag^+ ions are reduced efficiently by photoelectrons in under 10 ns. Without the photoelectrons present, the photoholes decay with a half-life of 0.27 s mainly due to their reaction with water. Therefore, formation of O_2 requires on the order of 1 s under simulated sunlight (AM 1.5 G).

However, additives that would not be found in an actual device can affect the dynamics, as shown dramatically in studies of the effects of electrolyte composition on dye-sensitized solar cells [12]. This is true also in water splitting, as replacing Ag^+ with Pt metal, deposited onto the TiO_2 surface, in the experiments of Tang et al. [11] decreased the hole half-life to 0.5 ms. Recent work by Cowan et al. applied simultaneous TA and photoelectrochemistry to a complete PEC cell made from TiO_2 NPs [4, 13]. This allows both reaction products and dynamics to be studied under an applied bias voltage, reproducing the conditions within an actual working device. No scavenger species are introduced, to avoid competing side-reactions or unwanted changes of the TiO_2 surface properties.

Without an applied bias, no photocurrent or gaseous product is produced and electrons and holes have roughly equal lifetimes [4]. This shows that electron–hole recombination is a primary factor limiting PEC efficiency. Under a positive bias, where the cell produces O_2 and H_2, greatly increased hole lifetimes are observed (Fig. 3) [4, 13]. Temperature has no observable effect on the hole lifetime, meaning that the activation energy for water oxidation is too small to be of consequence [13]. The main problem, therefore, is extremely slow kinetics due to the four-hole process required to form O_2. The applied bias affects the energies of the charge carriers and likely aids the diffusion of electrons away from holes. Improving spatial separation between charge carriers to maintain a larger fraction of long-lived holes can be achieved by several strategies, most critically controlling the size and shape of TiO_2 structures on nanometer length scales.

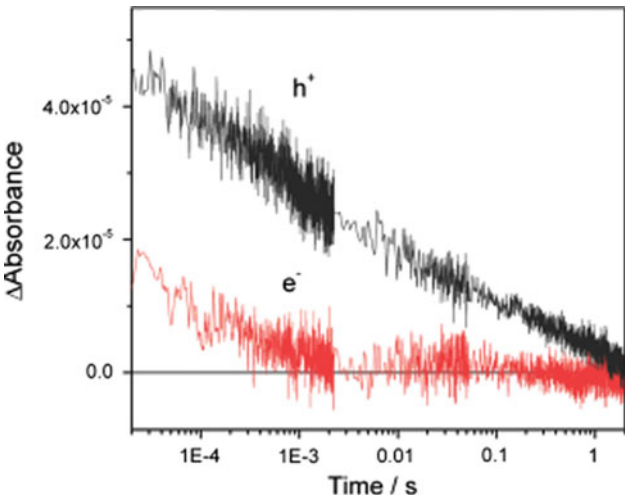

Fig. 3 Transient absorption signal decay for hole and electron probed at 460 and 900 nm, respectively, measured at a TiO_2 within a PEC cell containing 0.05 M NaOH/0.5 M $NaClO_4$ [13]. Under working conditions of positive bias (245 mV vs Ag/AgCl) and low excitation (50 μJ/cm^2, 355 nm), the hole greatly outlives the electron. Reprinted with permission from Cowan et al. [13]. Copyright 2011 American Chemical Society

3 Titania nanotubes

3.1 Properties

Given the problem of water splitting being much slower than electron–hole recombination, improving charge separation is vital to increasing yields from photocatalytic and PEC reactions. Can controlling the size and shape of TiO_2 on the nanoscale provide a path toward a solution? The electrical conductivity of a film made from a connected network of TiO_2 nanomaterials is limited by electron trapping to a far greater extent than single-crystalline bulk semiconductors [14]. Extensive theoretical modeling combined with careful experimentation has determined that the electron diffusion length in a film of TiO_2 NPs is ~10 μm [15]. For UV light, absorbed strongly by TiO_2, electron–hole pairs will be created at distances from the semiconductor particle surface that are within the diffusion length. If the electron can be transferred to another particle, the probability of which is influenced by the applied electric field (see previous section), and then, recombination can be avoided and the hole will remain available for chemistry. As we will see later, incorporating other materials into the TiO_2 particle network can extend the absorption range out to visible wavelengths, although the absorptivity in the visible often remains much weaker than in the UV. Weaker absorptivity requires that light be harvested over length scales, which may exceed the diffusion length, such that a greater number of electrons will recombine with holes before water oxidation can occur.

The efficiency of TiO_2 mesoporous films for water splitting also depends greatly on the degree of electrical connectivity within the film. Films made through sol–gel methods show better connectivity and an order of magnitude higher efficiency than films of sintered NPs [7]. Taken with the above results, this study suggests that a more conductive particle network can improve charge separation and potentially allow for more effective power conversion efficiency even when complete light harvesting requires distances longer than 10 μm. At the same time, holes have a diffusion length of only ~20 nm and thus must have ready access to the particle surface [16]. One type of nanostructure that satisfies all these constraints is the nanotube (NT), and as a result, interest in TiO_2 NTs has exploded in recent years [17–20].

3.2 Fabrication

A number of methods have been developed to form TiO_2 NTs, but the resulting materials are often of poor structural quality or have a tendency to form aggregates [21]. The most widely used procedure is currently potentiostatic anodization of Ti metal, first reported by Zwilling et al. [22]. Anodization is performed typically on thin (0.25 mm) high-purity Ti foils in a two-electrode electrochemical cell containing fluoride ions (Fig. 4). Titanium is used as the working electrode with Pt foil, the most stable choice for the counter electrode. An applied potential causes the formation of an array of hollow TiO_2 NTs that grows outward from the surface of the Ti foil (Fig. 5). The fact that the tubes are in a regular array oriented largely normal to the surface has attracted a lot of attention to this method. The electrolyte composition, anodization potential, and temperature during growth affect significantly the growth rate and the final dimensions of the NTs [17, 18, 20, 23, 24]. The resulting NTs are generally amorphous and require annealing after growth to form crystalline domains.

Mor et al. [25] reported the formation of 120-nm-long NTs with a wall thickness of 9 nm during anodization at

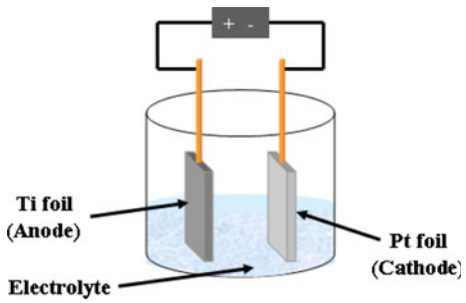

Fig. 4 Schematic diagram of the anodization set-up used to fabricate TiO_2 NT arrays. Reprinted with permission from Allam and Grimes [70]. Copyright 2009 American Chemical Society

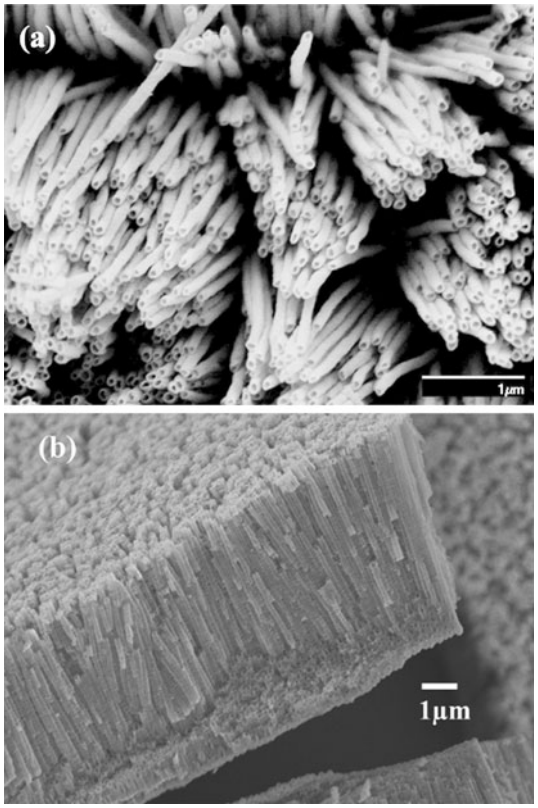

Fig. 5 Field emission scanning electron microscope images of TiO_2 NTs formed after anodizing Ti foil at 20 V for 20 h in formamide containing 0.2 M NH_4F, 1 M H_3PO_4, and 3 vol% H_2O: **a** top view, **b** cross-sectional view. Reprinted with permission from Allam and El-Sayed [29]. Copyright 2010 American Chemical Society

10 V in 50 °C electrolyte made from a mixture of HF and acetic acid. The tube length increased to 224 nm if the anodization was performed at 5 °C, but the wall thickness increased to 34 nm. Longer tubes were formed with less acidic electrolytes, in which TiO_2 dissolves more slowly [20]. Using a neutral electrolyte of 1 M Na_2SO_4 with 5 wt% NH_4F, NTs 3 μm in length were formed in 30 min of anodization at 20 V [26]. The wall thickness was ~10 nm, but the diameter of the tubes was larger at the bottom (100 nm) than at the top (~50 nm) due to the pH gradient that forms during anodization.

Producing longer NTs requires the use of organic solvent mixtures with low water content. As the solvent viscosity increases, ion mobility decreases, which slows the chemical dissolution of TiO_2 by fluoride [24]. Decreasing the water fraction also decreases the concentration of fluoride, so fewer reactive ions will be present at the top of the nanotube. The reduced dissolution rate allows higher potentials to be applied, so that Ti oxidation can occur more quickly. As a result, growth rates increase and longer tube structures can be formed. A more extensive discussion of the formation mechanism can be found in papers by Macak et al. [18] and Su and Zhou [20].

The exact NT dimensions depend on the kinetic balance that is established for a particular electrolyte composition and anodization potential. Yin et al. [24] observed growth rates as high as 100 μm/h in 0.09 M NH_4F in ethylene glycol containing 1 vol% H_2O, anodizing at 150 V and 20 °C. The outer diameter of the NTs was 300 nm. The growth rate dropped to <5 μm/h when the water content was increased to 10 vol%, but an outer diameter of 600 nm was obtained. Shankar et al. [23] reported tubes with length 223 μm, wall thickness 25 nm, and outer diameter 160 nm using 0.25 wt% NH_4F in ethylene glycol with 2 vol% H_2O. The NT growth, however, required 17 h at 60 V, with anodization at 80 V not leading to formation of NT structures. If more viscous solvents, such as polyethylene glycol, are used, the rate of dissolution is slowed to such an extent that partially crystalline NTs can form during anodization [21]. Although most studies have used NH_4F, there are recent reports of the successful use of ionic liquids as electrolytes which provides further possibilities to tune NT growth [27, 28].

Crystallization of the amorphous NTs into the photoactive anatase phase of TiO_2 begins at annealing temperatures of ~280 °C in a variety of atmospheres [30], with conversion to the rutile phase beginning at annealing temperatures above 500 °C [26, 29–31]. As the rutile phase is more dense than anatase, this phase transition is accompanied by significant degradation and cracking of the NT array [29, 32]. Incorporation of dopants/impurities from the electrolyte, such as P ions, into the TiO_2 can retard the anatase-to-rutile phase transition and allow higher annealing temperatures to be used [29].

3.3 Performance in water splitting

For both TiO_2 NPs and NTs, the size and phase of the crystalline domains as well as the connectivity between domains has a profound effect on the power conversion efficiency to produce hydrogen fuel from solar energy. Unannealed, amorphous samples have little to no ability to be used for water splitting [21]. Park et al. [33] compared directly 3-μm-long NTs with a 15-μm-thick film of NPs (P-25, a mixture of anatase and rutile TiO_2 phases), both samples annealed at 450 °C. In a PEC cell with 1 M KOH electrolyte, the photocurrent under an applied bias voltage is ~10 times greater for the NT array compared to the NP film. Decreasing the NT length lowered the photocurrent, as both the light absorption and surface area in contact with electrolyte decreased.

For a water splitting PEC cell, the efficiency (η) may be calculated from

$$\eta = \frac{(1.229\text{V} - V_{\text{bias}})I_{\text{p}}}{P} \quad (1)$$

where 1.229 V is the standard potential required to form H_2 and O_2 from H_2O, V_{bias} is the applied bias voltage, I_p is the measured photocurrent density in A/m^2, and P is the intensity of the incident light expressed in W/m^2 [19]. For broadband illumination under simulated AM 1.5 G sunlight, P is $\sim$1,000 W/m^2. Since pure TiO_2 has negligible absorptivity above 400 nm, efficiency is often calculated from the UV portion of the solar spectrum alone, typically 320–400 nm [34]. Care must be taken when comparing results that the measurements were taken under similar conditions. There is also a dependence of I_p on V_{bias}, although a plateau in I_p is typically reached resulting in a distinct optimal value for V_{bias} that maximizes η [7, 19].

There is a general trend toward increased cell performance as the temperature at which the NTs are annealed increases. This is expected due to greater crystallinity, which improves charge transport. Arrays of 7-μm-long NTs, whose structural properties are shown in Fig. 6, exhibit conversion efficiencies (Fig. 7) as high as 10 % under UV light (320–400 nm, filtered Xe arc lamp, 1,000 W/m^2) [29]. Interestingly, the optimum annealing temperature of 580 °C causes a reduction in the average grain size of the anatase phase and the appearance of the rutile phase. This may indicate that the anatase-to-rutile phase transition occurs more readily at the largest anatase grains. Control experiments on bare Ti foil show complete oxidation to rutile at the same temperature. As the substrate of Ti metal remains after anodization, this suggests that a significant portion of the rutile signal (Fig. 6) is originating from the oxidized substrate and not the NTs. Above 580 °C, the NT array is significantly damaged and η decreases.

Conversion efficiencies as high as 16.25 % have been reported [23]. This result was achieved with 30-μm-long

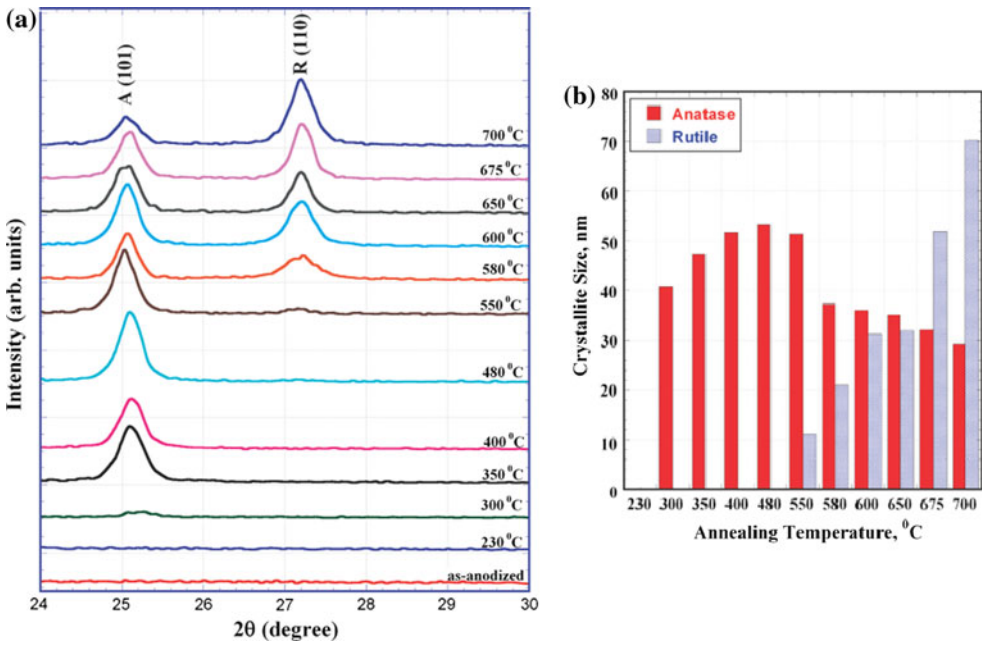

Fig. 6 Effects of annealing on crystallinity of 7-μm-long TiO_2 NTs formed after anodizing Ti foil at 20 V for 20 h in formamide containing 0.2 M NH_4F, 1 M H_3PO_4, and 3 vol% H_2O: **a** Glancing angle X-ray diffraction patterns and **b** corresponding crystallite sizes. The films are initially amorphous, with anatase (101) (*A*) and rutile (110) (*R*) phases forming after annealing [29]. Reprinted with permission from Allam and El-Sayed [29]. Copyright 2010 American Chemical Society

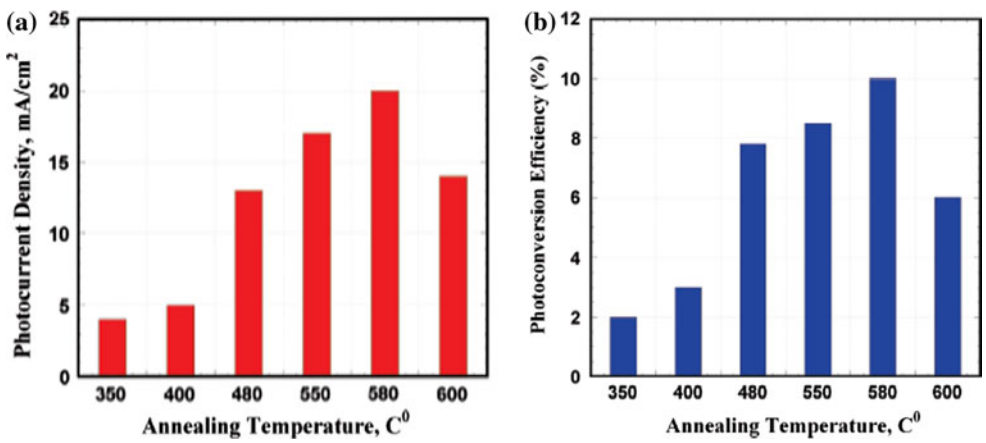

Fig. 7 **a** The steady-state photocurrent generated from 7-μm-long TiO_2 nanotube arrays under an applied voltage of 0.5 V (vs saturated Ag/AgCl) in 1 M KOH with respect to annealing temperature and **b** the corresponding photoconversion efficiencies under 320–400 nm light [29]. Reprinted with permission from Allam and El-Sayed [29]. Copyright 2010 American Chemical Society

NTs in 1 M KOH under light from a filtered Hg arc lamp (320–400 nm, 980 W/m^2). The optimal NT dimensions for water splitting, and the anodization and annealing conditions required to achieve them, are by no means established. With continuing improvements in NT fabrication and crystallization providing higher material quality and better size control, the balance between light harvesting and charge diffusion (Sect. 3.1) that makes the most efficient use of UV light will hopefully be achieved.

4 Composite nanotubes

Despite the advantages of TiO_2 as a material for solar energy conversion, the high (>3.0 eV) band gap still presents a significant drawback. Incorporating components with lower band gaps or lower-energy defect states into photoelectrodes can potentially improve conversion efficiency by extending the absorption edge into the visible region of the spectrum. Even in the case where UV photons are absorbed by TiO_2, placing TiO_2 in contact with a material with a lower-energy conduction-band edge may improve cell performance [35]. Electrons can transfer to lower-energy sites within the electrode, and the spatial separation of electron and hole reduces the rate of recombination.

Additional elements may be incorporated into NTs by anodizing Ti foil with an appropriately modified electrolyte. For example, we have recently fabricated TiO_2 NTs doped with Sr by using an aqueous electrolyte containing NH_4F, H_3PO_4, and $Sr(OH)_2$ [36]. Pure TiO_2 NTs, 1.2 μm long, displayed a maximum η of 0.2 % (in 1 M KOH under AM 1.5 G simulated sunlight, 1,000 W/m^2). By contrast, NTs of similar length (1.4 μm) with just 0.41 % Sr content were found to have a maximum η of 0.69 % under the same conditions. Compared with approaches that add $SrTiO_3$ to the surface of the NTs after anodization, incorporating Sr directly into the tube growth preserves the advantageous structural features of NTs.

Phosphorus-doped TiO_2 NTs have been formed by anodizing Ti foil in formamide containing NH_4F and H_3PO_4 [29]. This has the benefit of stabilizing the anatase phase allowing higher annealing temperatures to be used (see Sect. 3.3). X-ray photoelectron spectroscopy (XPS) revealed incorporated or doped P atoms, which was accompanied by a slightly redshifted absorption edge. The redshift was previously observed in P-doped sol–gel TiO_2 made by Xu et al. [37] with samples containing 16.7 % P having an absorption edge at 447 nm consistent with a band gap reduction of 0.43 eV. Density functional theory predicted a mixing of the O 2p states in the valence band of TiO_2 with P 3p states, causing the narrower band gap consistent with experimental results.

A similar approach has been used to form N-doped TiO_2 NTs. Shankar et al. performed anodization in an aqueous electrolyte of HF and NH_4NO_3 [38]. The N atoms were distributed inhomogeneously with a higher concentration near the tops of the tubes. The doped NTs showed a second absorption edge near 510 nm and produced roughly 5 times more photocurrent under broadband illumination (AM 1.5 G simulated sunlight). Similar absorption features were observed in N-doped TiO_2 thin films produced by DC magnetron sputtering [39, 40], where it was determined that the dopant gave rise to surface states above the TiO_2 valence band [39]. Although the surface states produce a PEC response to visible light, they can accelerate electron–hole recombination and decrease performance under UV light [40].

Li and Shang formed NTs using an electrolyte solution comprised on NH_4F, NH_4Cl, glycerin, and water [41]. The resulting NT array was ~500 μm long after 3 h of anodization. X-ray photoelectron spectra showed a sample enriched with N and F atoms, with some belonging to adsorbed species, while others were bonded to Ti in the crystal lattice. Annealing in an oxygen-free N_2 atmosphere preserved some of the F-containing and most of the N-containing species, yielding a sample with broad, weak absorption from 400 to 780 nm. Similar results were obtained by Liu et al. [42].

A very promising strategy for synthesizing composite NTs containing TiO_2 is anodizing metal alloys to form mixed metal oxides. Anodization has been reported on alloys of Ti with Fe [43], Cu [44], Pd [45], W [46], Al [47, 48], Mn [49], Nb [50, 51], and Zr [52] to successfully form NTs. Mor et al. [43] tested an array of Ti–Fe–O NTs as the photoanode for PEC water splitting, motivated by the lower band gap of Fe_2O_3. The most efficient material was obtained starting from a Ti foil containing 6.6 % Fe. The ~1.5-μm-long NTs were active at wavelengths out to ~600 nm, but no more than 7 % of absorbed photons at ~450 nm, where maximum visible light conversion efficiency was obtained, produced current. Photocurrent was lower if NTs with greater Fe content were used, possibly because of the low electron mobility in Fe_2O_3.

We have fabricated vertically oriented Ti–Nb–Zr–O mixed oxide NT arrays with wall thicknesses of 10 ± 2 nm [53]. This material showed enhanced power conversion efficiency for water splitting as compared to pure TiO_2 nanotubes (Fig. 8). Under UV light (filtered Xe arc lamp, 320–400 nm, 1,000 W/m^2) in 1 M KOH, the mixed metal oxides are ~17.5 % more efficient and require less applied bias. Oxides of Zr and Nb, formed on the surface of the NTs, may help to isolate electrons in the TiO_2 conduction band from species in solution, reducing recombination losses and consequently improving PEC efficiency.

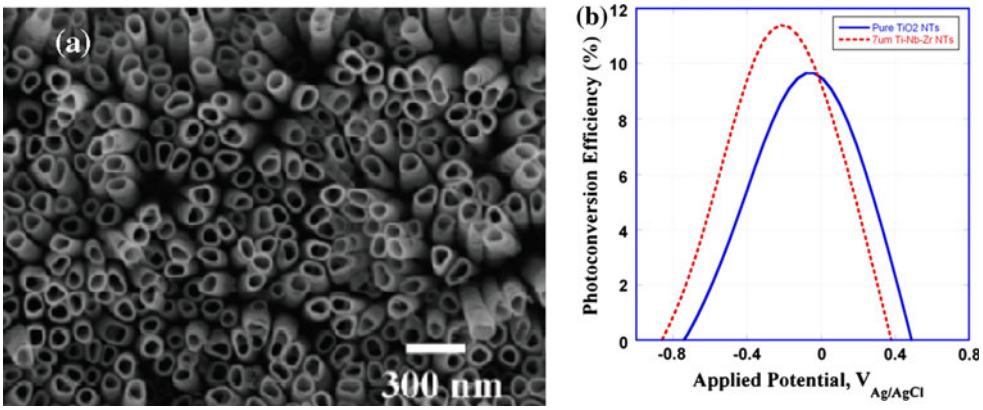

Fig. 8 **a** Field emission scanning electron microscope image of Ti–Nb–Zr mixed oxide NTs and **b** the UV power conversion efficiency of the mixed oxide NTs as compared to TiO_2 NTs of the same length (7 μm) [53]. Reprinted with permission from Allam et al. [53]. Copyright 2010 American Chemical Society

Recently, we have combined the use of metal alloys with doping to great effect [45]. We anodized Ti–Pd alloy, as Pd is an excellent catalyst that absorbs visible light, to form NTs 6 μm in length. The alloy NTs were then annealed in NH_3 to dope them with nitrogen. Increasing the annealing temperature to 550 °C caused a profound change in the X-ray photoelectron spectrum confirming the presence of Ti–O–N structures rather than unbonded nitrogen dopants. The Ti–Pd oxynitride NTs exhibited an absorption band edge redshifted to 577 nm and over 4 times greater power conversion efficiency compared to pure TiO_2 NTs.

Finally, it is worth noting that absorption properties can be modified greatly by the creation of large amounts of defect states without introducing dopants into the bulk. This was recently demonstrated by annealing TiO_2 NPs [54], nanowires [55], and NTs [55] in a hydrogen atmosphere. The H_2-treated TiO_2 absorbed visible light, turning gray or black depending on the annealing temperature. The mechanism is controversial. In the NP samples, the color change was attributed to a disorder-induced shift in the valence band position [54]; no such shift was measured for the nanowires and NTs [55]. The color change in the nanowires and NTs imparted only extremely weak visible light PEC activity but increased the UV response by a factor of 2 or more [55]. The increased UV activity was explained by the measured increase in carrier density following H_2 treatment, due to the resulting oxygen vacancies acting as electron donors. The vacancy states themselves, located within the band gap, are believed to be too high in energy and too electronically localized to be significantly active in water splitting.

5 Plasmonic effects in solar water splitting

As we have seen, methods that extend the absorption range of TiO_2 into the visible and produce PEC activity to visible light do so only weakly. In addition to increasing the absorptivity of the material itself, one can also increase the electric field strength to increase the number of photons absorbed. This can be done on the nanoscale by the use of noble-metal NPs that exhibit plasmonic effects [56, 57].

A surface plasmon resonance (SPR) is a collective oscillation of electrons confined to the surface of a metal NP. The lowest order effect gives rise to a local electric field due to a light-induced dipole (Fig. 9). At the surface of the NP, the dipole enhances the electric field to several orders of magnitude greater than the field of the light itself. This near-field enhancement can benefit a variety of optical processes. The energy of the SPR depends on multiple factors, such as the electronic properties of the metal, the dielectric properties of the surrounding medium, the size and shape of the NP, and the position of neighboring NPs. Only Ag, Au, and Cu possess SPRs that are always located in the visible or redder regions of the spectrum, but only Ag and Au are widely utilized due to their greater chemical stability.

Liu et al. [42] evaporated a Au film onto a F- and N-doped TiO_2 NT array, forming islands of metal with plasmonic properties of NPs. A significant enhancement in photocurrent compared to an array not containing Au was

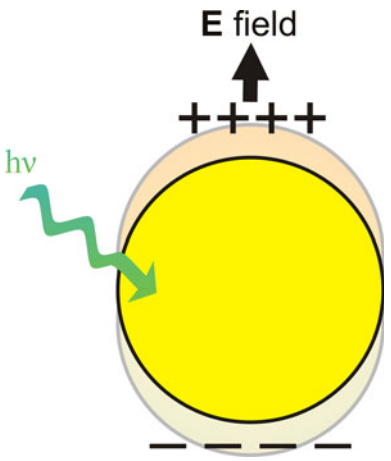

Fig. 9 Surface plasmon resonance (SPR) in a metal nanoparticle

reported when a visible light source was used. The authors attributed this to a local field enhancement at wavelengths that excited the SPR of Au and were also absorbed by TiO_2. The absorption spectrum of the TiO_2 NTs contained a broad tail in the visible region of the spectrum due to the impurity doping. Photocurrent caused by visible light, 1–2 orders of magnitude higher than that produced by the NTs without Au, was still lower than photocurrent produced by UV light. In fact, photocurrent caused by UV absorption was significantly reduced by Au NPs, explained by the authors as the effect of reduced absorption by TiO_2 and less oxide surface area in contact with the electrolyte.

It is known that Au [58, 59] and Ag [60] NPs can act as sensitizers, injecting electrons into TiO_2 after absorbing visible light. Liu et al. [42] did not observe photocurrent under visible light, however, if Au NPs were adsorbed on undoped TiO_2 that lacked visible light absorption. This result shows that the combination of doping and the plasmonic effect are likely responsible for the enhanced current in PEC cells. Finite-difference time-domain (FDTD) simulations of the Au/TiO_2 film show regions of enhanced electric field strength in the gaps between closely spaced Au NPs, consistent with the observed plasmonic effect [42]. Due to the regions of enhanced field, electron–hole pairs are created near the TiO_2 surface thus facilitating water oxidation by the photoholes.

Similar effects were seen for Ag nanocubes, prepared through colloidal synthesis and deposited on N-doped TiO_2 NTs [61]. Ingram and Linic observed current enhancements of an order of magnitude in a Ag/TiO_2 composite water splitting cell when light from 400 to 500 nm was used. Light in this range of wavelengths is resonant with both the absorption from the Ag SPR and the N dopants in TiO_2. A similar PEC cell, constructed using Au nanospheres instead of Ag nanocubes, showed little or no enhancement because the SPR did not overlap with the absorption of their NTs. At 370 nm, on the edge of the SPR absorption but still resonant with TiO_2 absorption, an enhancement factor between 3 and 4 was still observed. Whether the Ag nanocubes caused a reduction in current at lower wavelengths, as occurred with the Au film used by Liu et al. [42], was not reported.

In addition to FDTD simulations, which showed significantly enhanced electric fields at the sharp corners of the nanocubes, power dependence studies helped to confirm the plasmonic nature of the photocurrent enhancement [61]. In studies of the TiO_2(110) surface using a beam of electrons, which have shallow penetration depths, to excite electron–hole pairs near the surface, the concentration of holes depends linearly on the excitation intensity [62]. The current generated through water splitting using the plasmonic photoelectrode also depended linearly on the excitation intensity (of visible light, in this case), suggesting

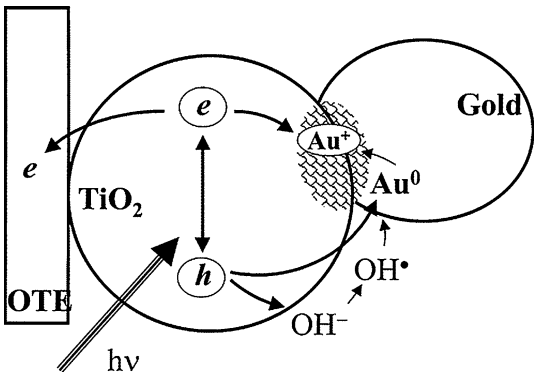

Fig. 10 Proposed reaction scheme for the decomposition of Au NPs on TiO_2 surfaces in the presence of OH^-. Reprinted with permission from Subramanian et al. [63]. Copyright 2001 American Chemical Society

that holes were being produced near the surface in this system as well [61]. Near-surface excitation with visible light is due to the locally enhanced electric field caused by the plasmonic effect. For the PEC without Ag nanocubes, the power dependence is nonlinear and consistent with excitation deeper in the bulk of TiO_2 [61, 62].

For plasmonic effects from noble-metal NPs to be fully utilized in water splitting PEC cells, the NPs must be chemically stable during extended use. Although Subramanian et al. [63] reported enhanced photocurrent after depositing Au NPs onto TiO_2 films, the current dropped rapidly during 60 min of continuous illumination. The working conditions were in 0.05 M NaOH solution under UV light. Changes in the UV–visible absorption spectrum of the electrode were consistent with the gradual incorporation of ions, possibly Au^+, in the TiO_2 matrix [63, 64]. X-ray absorption fine structure measurements confirmed the accumulation of Au atoms or ions [64]. The proposed mechanism (Fig. 10) was oxidation of hydroxide ions by photoholes to form highly reactive OH radicals, which could react with Au metal to form Au ions. One possible remedy is the presence of an electron donor, such as a metal chloride, in contact with the metal particle to neutralize metal ions and stabilize the NPs [60]. Another promising approach is metal core/oxide-shell NPs [65–68] to prevent oxidation of the metal NPs by radicals in solution.

6 Conclusions

In this review, we have presented some of the highlights in the area of research dedicated to developing a practical PEC system to turn solar energy and water into hydrogen and oxygen using the highly abundant and chemically stable material TiO_2. Performing TA spectroscopy on PEC cells under operating conditions reveals dynamics on

multiple timescales, providing further mechanistic understanding. Controlled anodization of metal foils to produce metal oxide NTs has the potential to develop highly efficient photoelectrodes for "water splitting", incorporating dopants or phases of other materials to improve charge separation and light harvesting. Finally, plasmonic NPs, incorporated into the photoelectrodes, can further improve light harvesting provided that issues of chemical stability can be addressed and performance under UV light is not adversely affected.

A considerable challenge will be to measure and interpret the dynamics of photoexcited charge carriers in 1D nanostructures such as TiO_2 NTs. The main experimental issue is that anodization of metal foils produces an NT array atop an opaque metal foil, preventing the measurement of light transmission (and absorption). Considerable effort has been invested in forming ordered NT arrays on transparent conductive substrates for photovoltaic systems [19], producing transmissive electrodes that would enable many spectroscopic measurements. Alternatively, TA could be measured through diffuse reflectance from an opaque sample as demonstrated on dye-sensitized solar cells [69]. Ultimately, materials synthesis, spectroscopy, and modeling and computational studies should inform each other and influence their research directions, pointing the way toward increasingly more efficient and practical systems for solar water splitting.

Acknowledgments The authors would like to thank the financial support of the Office of Basic Energy Sciences of the US Department of Energy under contract number DE-FG02-97ER14799.

References

1. Lewis NS, Crabtree G, Nozik AJ, Wasielewski MR, Alivisatos AP (2006) Basic research needs for solar energy utilization. US Department of Energy, Washington
2. Fukushima A, Hasimoto K, Watanabe T (1999) TiO_2 photocatalysis: fundamentals and applications, 1st edn. BKC, Tokyo
3. Fujishima A, Honda K (1972) Electrochemical photolysis of water at a semiconductor electrode. Nature 238(5358):37–38
4. Cowan AJ, Tang J, Leng W, Durrant JR, Klug DR (2010) Water splitting by nanocrystalline TiO_2 in a complete photoelectrochemical cell exhibits efficiencies limited by charge recombination. J Phys Chem C 114(9):4208–4214
5. Grätzel M (2005) Solar energy conversion by dye-sensitized photovoltaic cells. Inorg Chem 44(20):6841–6851
6. Chen X, Shen S, Guo L, Mao SS (2010) Semiconductor-based photocatalytic hydrogen generation. Chem Rev 110(11):6503–6570
7. Hartmann P, Lee D-K, Smarsly BM, Janek J (2010) Mesoporous TiO_2: comparison of classical sol−gel and nanoparticle based photoelectrodes for the water splitting reaction. ACS Nano 4(6):3147–3154
8. Gueymard CA, Myers D, Emery K (2002) Proposed reference irradiance spectra for solar energy systems testing. Sol Energy 73(6):443–467
9. Tamaki Y, Furube A, Murai M, Hara K, Katoh R, Tachiya M (2007) Dynamics of efficient electron-hole separation in TiO_2 nanoparticles revealed by femtosecond transient absorption spectroscopy under the weak-excitation condition. Phys Chem Chem Phys 9(12):1453–1460
10. Murai M, Tamaki Y, Furube A, Hara K, Katoh R (2007) Reaction of holes in nanocrystalline TiO_2 films evaluated by highly sensitive transient absorption spectroscopy. Catal Today 120(2):214–219
11. Tang J, Durrant JR, Klug DR (2008) Mechanism of photocatalytic water splitting in TiO_2. reaction of water with photoholes, importance of charge carrier dynamics, and evidence for four-hole chemistry. J Am Chem Soc 130(42):13885–13891
12. Listorti A, O'Regan B, Durrant JR (2011) Electron transfer dynamics in dye-sensitized solar cells. Chem Mater 23(15):3381–3399
13. Cowan AJ, Barnett CJ, Pendlebury SR, Barroso M, Sivula K, Grätzel M, Durrant JR, Klug DR (2011) Activation energies for the rate-limiting step in water photooxidation by nanostructured α-Fe_2O_3 and TiO_2. J Am Chem Soc 133(26):10134–10140
14. de Jongh PE, Vanmaekelbergh D (1996) Trap-limited electronic transport in assemblies of nanometer-size TiO_2 particles. Phys Rev Lett 77(16):3427
15. Leng WH, Barnes PRF, Juozapavicius M, O'Regan BC, Durrant JR (2010) Electron diffusion length in mesoporous nanocrystalline TiO_2 photoelectrodes during water oxidation. J Phys Chem Lett 1(6):967–972
16. Grimes CA, Varghese OK, Ranjan S (2008) Light, water, hydrogen: the solar generation of hydrogen by water photoelectrolysis. Springer US, Boston
17. Grimes CA (2007) Synthesis and application of highly ordered arrays of TiO_2 nanotubes. J Mater Chem 17(15):1451–1457
18. Macak JM, Tsuchiya H, Ghicov A, Yasuda K, Hahn R, Bauer S, Schmuki P (2007) TiO_2 nanotubes: self-organized electrochemical formation, properties and applications. Curr Opin Solid State Mater Sci 11(1–2):3–18
19. Shankar K, Basham JI, Allam NK, Varghese OK, Mor GK, Feng X, Paulose M, Seabold JA, Choi K-S, Grimes CA (2009) Recent advances in the use of TiO_2 nanotube and nanowire arrays for oxidative photoelectrochemistry. J Phys Chem C 113(16):6327–6359
20. Su Z, Zhou W (2011) Formation, morphology control and applications of anodic TiO_2 nanotube arrays. J Mater Chem 21(25):8955–8970
21. Allam NK, Grimes CA (2009) Room temperature one-step polyol synthesis of anatase TiO_2 nanotube arrays: photoelectrochemical properties. Langmuir 25(13):7234–7240
22. Zwilling V, Darque-Ceretti E, Boutry-Forveille A, David D, Perrin MY, Aucouturier M (1999) Structure and physicochemistry of anodic oxide films on titanium and TA6V alloy. Surf Interface Anal 27(7):629–637
23. Shankar K, Mor GK, Prakasam HE, Yoriya S, Paulose M, Varghese OK, Grimes CA (2007) Highly-ordered TiO_2 nanotube arrays up to 220 μm in length: use in water photoelectrolysis and dye-sensitized solar cells. Nanotechnology 18(6):065707
24. Yin H et al (2010) The large diameter and fast growth of self-organized TiO_2 nanotube arrays achieved via electrochemical anodization. Nanotechnology 21(3):035601
25. Mor GK, Shankar K, Paulose M, Varghese OK, Grimes CA (2004) Enhanced photocleavage of water using Titania nanotube arrays. Nano Lett 5(1):191–195
26. Lockman Z, Ismail S, Sreekantan S, Schmidt-Mende L, MacManus-Driscoll JL (2010) The rapid growth of 3 μm long Titania nanotubes by anodization of titanium in a neutral electrochemical bath. Nanotechnology 21(5):055601

27. Li H, Qu J, Cui Q, Xu H, Luo H, Chi M, Meisner RA, Wang W, Dai S (2011) TiO_2 nanotube arrays grown in ionic liquids: high-efficiency in photocatalysis and pore-widening. J Mater Chem 21(26):9487–9490
28. Wender H, Feil AF, Diaz LB, Ribeiro CS, Machado GJ, Migowski P, Weibel DE, Dupont J, Teixeira SrR (2011) Self-organized TiO_2 nanotube arrays: synthesis by anodization in an ionic liquid and assessment of photocatalytic properties. ACS Appl Mater Interfaces 3(4):1359–1365
29. Allam NK, El-Sayed MA (2010) Photoelectrochemical water oxidation characteristics of anodically fabricated TiO_2 nanotube arrays: structural and optical properties. J Phys Chem C 114(27): 12024–12029
30. Varghese OK, Gong D, Paulose M, Grimes CA, Dickey EC (2003) Crystallization and high-temperature structural stability of titanium oxide nanotube arrays. J Mater Res 18(01):156–165
31. Sun Y, Yan K, Wang G, Guo W, Ma T (2011) Effect of annealing temperature on the hydrogen production of TiO_2 nanotube arrays in a two-compartment photoelectrochemical cell. J Phys Chem C 115(26):12844–12849
32. Hardcastle FD, Ishihara H, Sharma R, Biris AS (2011) Photo-electroactivity and Raman spectroscopy of anodized titania (TiO_2) photoactive water-splitting catalysts as a function of oxygen-annealing temperature. J Mater Chem 21(17):6337–6345
33. Park JH, Kim S, Bard AJ (2005) Novel carbon-doped TiO_2 nanotube arrays with high aspect ratios for efficient solar water splitting. Nano Lett 6(1):24–28
34. Varghese OK, Grimes CA (2008) Appropriate strategies for determining the photoconversion efficiency of water photoelectrolysis cells: a review with examples using titania nanotube array photoanodes. Sol Energy Mater Sol Cells 92(4):374–384
35. Im JS, Lee SK, Lee Y-S (2011) Cocktail effect of Fe_2O_3 and TiO_2 semiconductors for a high performance dye-sensitized solar cell. Appl Surf Sci 257(6):2164–2169
36. Hamedani HA, Allam NK, Garmestani H, El-Sayed MA (2011) Electrochemical fabrication of strontium-doped TiO_2 nanotube array electrodes and investigation of their photoelectrochemical properties. J Phys Chem C 115(27):13480–13486
37. Xu L, Tang C-Q, Qian J, Huang Z-B (2010) Theoretical and experimental study on the electronic structure and optical absorption properties of P-doped TiO_2. Appl Surf Sci 256(9):2668–2671
38. Shankar K, Tep KC, Mor GK, Grimes CA (2006) An electrochemical strategy to incorporate nitrogen in nanostructured TiO_2 thin films: modification of bandgap and photoelectrochemical properties. J Phys D Appl Phys 39(11):2361–2366
39. Sakthivel S, Janczarek M, Kisch H (2004) Visible light activity and photoelectrochemical properties of nitrogen-doped TiO_2. J Phys Chem B 108(50):19384–19387
40. Lindgren T, Mwabora JM, Avendaño E, Jonsson J, Hoel A, Granqvist C-G, Lindquist S-E (2003) Photoelectrochemical and optical properties of nitrogen doped titanium dioxide films prepared by reactive DC magnetron sputtering. J Phys Chem B 107(24):5709–5716
41. Li Q, Shang JK (2009) Self-organized nitrogen and fluorine co-doped titanium oxide nanotube arrays with enhanced visible light photocatalytic performance. Environ Sci Technol 43(23): 8923–8929
42. Liu Z, Hou W, Pavaskar P, Aykol M, Cronin SB (2011) Plasmon resonant enhancement of photocatalytic water splitting under visible illumination. Nano Lett 11(3):1111–1116
43. Mor GK, Prakasam HE, Varghese OK, Shankar K, Grimes CA (2007) Vertically oriented Ti−Fe−O nanotube array films: toward a useful material architecture for solar spectrum water photoelectrolysis. Nano Lett 7(8):2356–2364
44. Mor GK, Varghese OK, Wilke RHT, Sharma S, Shankar K, Latempa TJ, Choi K-S, Grimes CA (2008) p-Type Cu−Ti−O nanotube arrays and their use in self-biased heterojunction photoelectrochemical diodes for hydrogen generation. Nano Lett 8(7):1906–1911
45. Allam NK, Poncheri AJ, El-Sayed MA (2011) Vertically oriented Ti–Pd mixed oxynitride nanotube arrays for enhanced photoelectrochemical water splitting. ACS Nano 5(6):5056–5066
46. Nah Y-C, Ghicov A, Kim D, Berger S, Schmuki P (2008) TiO_2−WO_3 composite nanotubes by alloy anodization: growth and enhanced electrochromic properties. J Am Chem Soc 130(48): 16154–16155
47. Bayoumi FM, Ateya BG (2006) Formation of self-organized titania nano-tubes by dealloying and anodic oxidation. Electrochem Commun 8(1):38–44
48. Berger S, Tsuchiya H, Schmuki P (2008) Transition from nanopores to nanotubes: self-ordered anodic oxide structures on titanium−aluminides. Chem Mater 20(10):3245–3247
49. Mohapatra SK, Raja KS, Misra M, Mahajan VK, Ahmadian M (2007) Synthesis of self-organized mixed oxide nanotubes by sonoelectrochemical anodization of Ti-8Mn alloy. Electrochim Acta 53(2):590–597
50. Ghicov A, Aldabergenova S, Tsuchyia H, Schmuki P (2006) TiO_2–Nb_2O_5 nanotubes with electrochemically tunable morphologies. Angew Chem Int Ed 45(42):6993–6996
51. Dongyan D et al (2009) Anodic fabrication and bioactivity of Nb-doped TiO_2 nanotubes. Nanotechnology 20(30):305103
52. Yasuda K, Schmuki P (2007) Electrochemical formation of self-organized zirconium titanate nanotube multilayers. Electrochem Commun 9(4):615–619
53. Allam NK, Alamgir F, El-Sayed MA (2010) Enhanced photoassisted water electrolysis using vertically oriented anodically fabricated Ti−Nb−Zr−O mixed oxide nanotube arrays. ACS Nano 4(10):5819–5826
54. Chen X, Liu L, Yu PY, Mao SS (2011) Increasing solar absorption for photocatalysis with black hydrogenated titanium dioxide nanocrystals. Science 331(6018):746–750
55. Wang G, Wang H, Ling Y, Tang Y, Yang X, Fitzmorris RC, Wang C, Zhang JZ, Li Y (2011) Hydrogen-treated TiO_2 nanowire arrays for photoelectrochemical water splitting. Nano Lett 11(7): 3026–3033
56. Jain PK, Huang X, El-Sayed IH, El-Sayed MA (2008) Noble metals on the nanoscale: optical and photothermal properties and some applications in imaging, sensing, biology, and medicine. Acc Chem Res 41(12):1578–1586
57. Jain PK, El-Sayed MA (2010) Plasmonic coupling in noble metal nanostructures. Chem Phys Lett 487(4–6):153–164
58. Du L, Furube A, Yamamoto K, Hara K, Katoh R, Tachiya M (2009) Plasmon-induced charge separation and recombination dynamics in gold−TiO_2 nanoparticle systems: dependence on TiO_2 particle size. J Phys Chem C 113(16):6454–6462
59. Furube A, Du L, Hara K, Katoh R, Tachiya M (2007) Ultrafast plasmon-induced electron transfer from gold nanodots into TiO_2 nanoparticles. J Am Chem Soc 129(48):14852–14853
60. Yu J, Dai G, Huang B (2009) Fabrication and characterization of visible-light-driven plasmonic photocatalyst Ag/AgCl/TiO_2 nanotube arrays. J Phys Chem C 113(37):16394–16401
61. Ingram DB, Linic S (2011) Water splitting on composite plasmonic-metal/semiconductor photoelectrodes: evidence for selective plasmon-induced formation of charge carriers near the semiconductor surface. J Am Chem Soc 133(14):5202–5205
62. Zhang Z, Yates JT (2010) Direct observation of surface-mediated electron−hole pair recombination in TiO_2(110). J Phys Chem C 114(7):3098–3101
63. Subramanian V, Wolf E, Kamat PV (2001) Semiconductor−metal composite nanostructures. To what extent do metal nanoparticles improve the photocatalytic activity of TiO_2 films? J Phys Chem B 105(46):11439–11446

64. Lahiri D, Subramanian V, Shibata T, Wolf EE, Bunker BA, Kamat PV (2003) Photoinduced transformations at semiconductor/metal interfaces: X-ray absorption studies of titania/gold films. J Appl Phys 93(5):2575–2582
65. Hirakawa T, Kamat PV (2005) Charge separation and catalytic activity of $Ag@TiO_2$ core−shell composite clusters under uv−irradiation. J Am Chem Soc 127(11):3928–3934
66. Sakai H, Kanda T, Shibata H, Ohkubo T, Abe M (2006) Preparation of highly dispersed core/shell-type titania nanocapsules containing a single Ag nanoparticle. J Am Chem Soc 128(15): 4944–4945
67. Awazu K, Fujimaki M, Rockstuhl C, Tominaga J, Murakami H, Ohki Y, Yoshida N, Watanabe T (2008) A plasmonic photocatalyst consisting of silver nanoparticles embedded in titanium dioxide. J Am Chem Soc 130(5):1676–1680
68. Chuang H-Y, Chen D-H (2009) Fabrication and photocatalytic activities in visible and UV light regions of $Ag@TiO_2$ and $NiAg@TiO_2$ nanoparticles. Nanotechnology 20(10):105704
69. Furube A, Wang Z-S, Sunahara K, Hara K, Katoh R, Tachiya M (2010) Femtosecond diffuse reflectance transient absorption for dye-sensitized solar cells under operational conditions: effect of electrolyte on electron injection. J Am Chem Soc 132(19):6614–6615
70. Allam NK, Grimes CA (2009) Effect of rapid infrared annealing on the photoelectrochemical properties of anodically fabricated TiO_2 nanotube arrays. J Phys Chem C 113(19):7996–7999